Giant (12 x 12) and (4 x 8) reconstructions of the 6 H -SiC(0001) surface obtained by progressive enrichment in Si atoms

David Martrou, Thomas Leoni, Florian Chaumeton, Fabien Castanié, Sebastien Gauthier, Xavier Bouju

Rapid Communications

Giant (12×12) and (4×8) reconstructions of the 6*H*-SiC(0001) surface obtained by progressive enrichment in Si atoms

David Martrou,[1,*] Thomas Leoni,[1,†] Florian Chaumeton,[1,2] Fabien Castanié,[1,2] Sébastien Gauthier,[1] and Xavier Bouju[1]
[1]*NanoSciences Group, CEMES, CNRS UPR 8011, 29 rue J. Marvig, 31055 Toulouse, France*
[2]*Université de Toulouse, UPS, 29 rue J. Marvig, F-31055 Toulouse, France*

(Received 23 November 2017; published 23 February 2018)

Silicon carbide (SiC) is nowadays a major material for applications in high power electronics, quantum optics, or nitride semiconductors growth. Mastering the surface of SiC substrate is crucial to obtain reproducible results. Previous studies on the 6*H*-SiC(0001) surface have determined several reconstructions, including the $(\sqrt{3}\times\sqrt{3})$-*R*30° and the (3×3). Here, we introduce a process of progressive Si enrichment that leads to the formation of two reconstructions, the giant (12×12) and the (4×8). From electron diffraction and tunneling microscopy completed by molecular dynamics simulations, we build models introducing a type of Si adatom bridging two Si surface atoms. Using these Si bridges, we also propose a structure for two other reconstructions, the $(2\sqrt{3}\times2\sqrt{3})$-*R*30° and the $(2\sqrt{3}\times2\sqrt{13})$. We show that five reconstructions follow each other with Si coverage ranging from 1 and 1.444 monolayer. This result opens the way to greatly improve the control of 6*H*-SiC(0001) at the atomic scale.

DOI: 10.1103/PhysRevB.97.081302

The Si terminated 6*H*-SiC(0001) surface has been widely studied since 1989 [1], and various reconstructions after Si exposure have been observed mainly by reflection high energy electron diffraction (RHEED), low-energy electron diffraction (LEED), grazing-incidence small-angle x-ray scattering (GISAX), and STM. The most common ones are the $(\sqrt{3}\times\sqrt{3})$-*R*30° [1–6] and the (3×3) [4,7–10] with Si adatom coverages of 1/3 and 13/9 monolayer (ML) over the Si atomic plane of the 6*H*-SiC(0001) surface. Between these two extremal values, the (6×6) [11,12], the $(2\sqrt{3}\times2\sqrt{3})$-*R*30° [13], and the $(2\sqrt{3}\times2\sqrt{13})$ [14] have been more rarely observed. Among all these Si-rich reconstructions, only the atomic structures of the $(\sqrt{3}\times\sqrt{3})$-*R*30° and the (3×3) have been clearly identified and validated from GISAX or LEED experiments and density functional theory (DFT) calculations [6,10]. In particular, Starke *et al.* showed that the (3×3) is terminated by silicon pyramids lying on one monolayer of Si adatoms [9]. The experimental process applied in these pioneering studies is based on two steps: deposition of an excess of Si atoms on the SiC surface followed by an annealing with *in situ* monitoring by LEED or RHEED. The observed reconstructions seem to be very sensitive to the parameters of the annealing, and the surfaces present generally many defects. Furthermore, there is no experimental process to control sequentially the different reconstructions of the surface.

In this paper, we propose a procedure based on a progressive enrichment in Si that allows us to better control the various reconstructions of the 6*H*-SiC(0001) surface. Doing so, we identify two reconstructions, namely the (12×12) and the (4×8) which are intermediate in terms of silicon coverage between the $(\sqrt{3}\times\sqrt{3})$-*R*30° and the (3×3). From RHEED and STM results, we build atomic models introducing a type of Si adatom in the bridge position between two Si surface atoms. We then perform molecular dynamics (MD) to check their stability at high temperature [15–18]. The choice of MD is dictated by the large number of atoms to consider, which prohibits the use of DFT calculations.

After preparing the 6*H*-SiC(0001) surface in a dedicated UHV equipment [16,19,20], the process of Si enrichment is started with series of cycles consisting in (1) Si deposition at $T_{\text{substrate}} = 830\,^{\circ}\text{C}$ during 3 min with a beam equivalent pressure of 6×10^{-10} Torr ($T_{\text{Si}} = 1250\,^{\circ}\text{C}$) and (2) an annealing at the same temperature during 15 mn. Between two and five cycles are needed to reach the $(\sqrt{3}\times\sqrt{3})$-*R*30° reconstruction.

Performing three more cycles leads to the modification of the RHEED pattern with multifold periodicity along the $\langle 1\,0\,\bar{1}\,0\rangle$ axis with weak fractional streaks and high background intensity. This RHEED pattern appears more clearly when the substrate temperature is decreased below 600 °C. Its periodicity is determined from the diagram shown in Fig. 1(a) obtained by summation of RHEED images within an angular domain of ±5° around a $[1\,0\,\bar{1}\,0]$ direction. The presence of the fractional streaks of order 5/12, 7/12, and 11/12 indicates a 12-fold periodicity along the $\langle 1\,0\,\bar{1}\,0\rangle$ axis. STM image acquired on this surface [Fig. 1(b)] presents areas with a regular pattern. The surface cell is oriented along the $\langle 1\,0\,\bar{1}\,0\rangle$ axis and its size is $a = b = 33 \pm 4$ Å corresponding to 11 ± 1 SiC bulk cell parameter ($a_{\text{SiC}} = b_{\text{SiC}} = 3.095$ Å). These observations indicate that the surface cell is $(12\times12) \parallel ([1\,0\,\bar{1}\,0],[0\,1\,\bar{1}\,0])$ with a surface cell parameter $a = b = 12 \times a_{\text{SiC}} = 37.14$ Å.

To determine the atomic structure of this reconstruction, we assume that the atoms observed by STM are the Si top adatoms as for the $(\sqrt{3}\times\sqrt{3})$-*R*30° and the (3×3) reconstructed surfaces [9]. They are in sp^3 configuration with three nearest neighbors of the Si underlayer and one dangling bond normal to the surface. Starting from their experimental positions, atomic

*Corresponding author: david.martrou@cemes.fr
†Present address: Aix Marseille Univ, CNRS, CINaM, UMR 7325, Marseille, France.

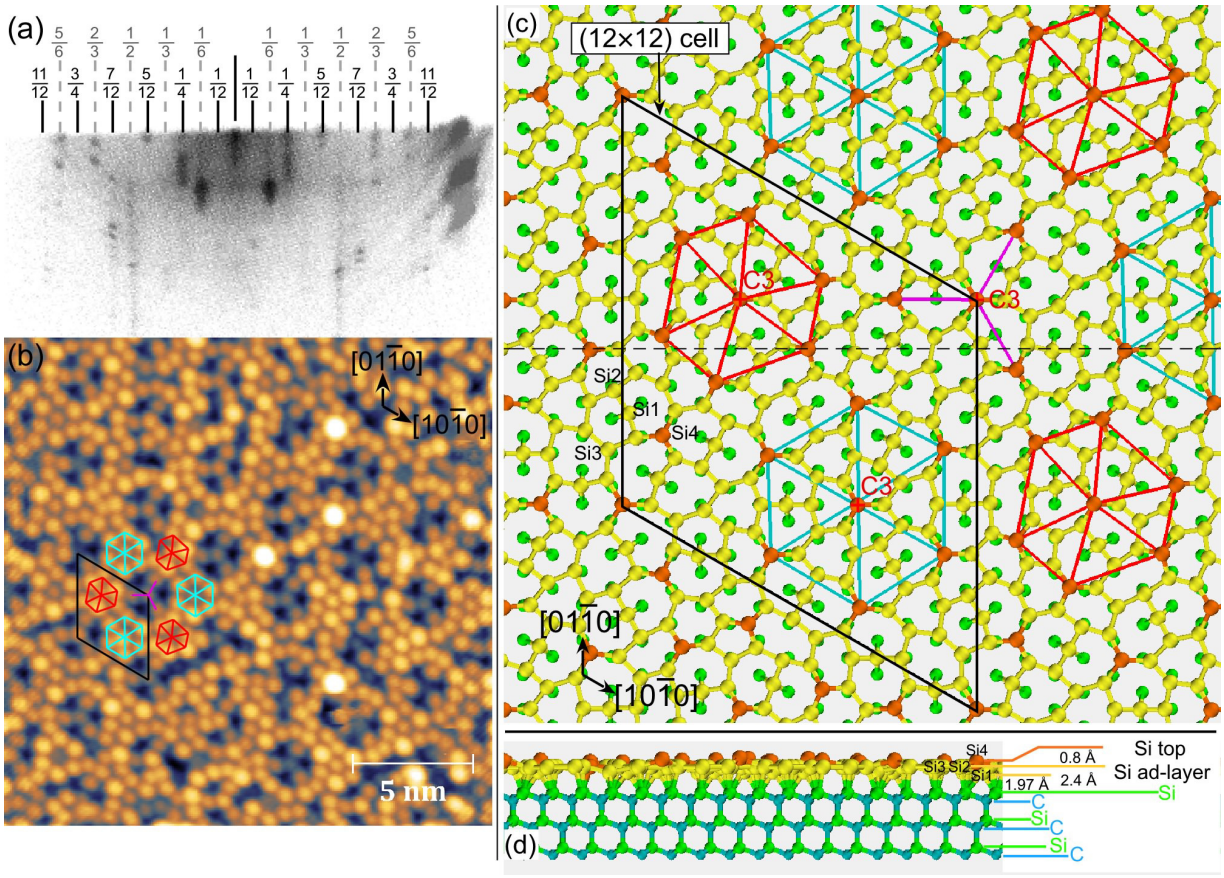

FIG. 1. The (12×12) reconstructed surface of 6*H*-SiC(0001): (a) RHEED pattern aligned along the [1 0 $\bar{1}$ 0] direction, (b) STM topography image acquired at $V_{\text{sample}} = -3.2$ V and $I = 40$ pA, (c) top view, and (d) cross section along the black dashed line of the atomic structure relaxed at 300 K. Si1, Si2, and Si3 adatoms in the first adlayer are in yellow, Si4 topmost adatoms on this first adlayer are in orange, Si atoms of the SiC(0001) bulk are in green, and C atoms are in blue. Pink, blue, and red lines highlight the local structures with threefold symmetry axis (C3) that are superimposed onto the STM topography.

models are built by adding Si adatoms with four first nearest neighbors in the first adlayer between the Si surface of the 6*H*-SiC(0001) crystal and the Si top adatoms. The stability of the structure at various temperatures is then checked by MD using the Tersoff potentials with parameters for Si and C identical to the original ones [16,17]. The model stable at 900 K, presented in Figs. 1(c) and 1(d), has 7/8 ML first adlayer Si adatoms (yellow) and 1/8 ML Si top adatoms in the second adlayer (orange), leading to a total of 144 additional Si adatoms by (12×12) unit cell.

The first adlayer Si adatoms can be classified in three types as shown in Fig. 1(c):

(i) Si1 are in a bridge position between two Si atoms of the 6*H*-SiC(0001) surface and are bound to these two Si surface atoms and to two Si adatoms,

(ii) Si2 are distorted sp^3 tetragonal Si atoms, bound to one Si surface atom and to three Si adatoms,

(iii) Si3 are sp^3 Si atoms in a sp^2-like geometrical configuration, bound to one Si surface atom and to three Si adatoms.

Si2 and Si3 appear in the model of the (3×3) reconstruction [9]. In contrast, the Si1 do not appear in the models of the two known ($\sqrt{3}\times\sqrt{3}$)-*R*30° and (3×3) reconstructions. These Si adatom configurations are at the basis of the structures presented in this paper.

The Si4 topmost adatoms form three local organizations with threefold rotation axis named C3 in Fig. 1(c): (1) a regular centered hexagon highlighted in blue, (2) a distorted centered hexagon in red, and (3) a three branches star in magenta. As shown in Fig. 1(a), the calculated positions of the Si4 top adatoms in these local structures fit perfectly the experimental image and in particular the distorted hexagon in red.

Continuing the surface enrichment with two more cycles leads to a RHEED pattern with twofold and threefold periodicities along the $\langle 1\,0\,\bar{1}\,0\rangle$ and $\langle 1\,2\,\bar{3}\,0\rangle$ axis. The threefold periodicities are characteristic of the (3×3) reconstructed surface, while the twofold streaks indicate the presence of another reconstruction. These reconstructions are observed on STM images in Fig. 2: (a) and (b) show the new reconstruction while in (c) the (3×3) reconstruction (black diamond) is present close to the new one (red diamond). This latter is formed by lines of Si atom pairs aligned along the [1 2 $\bar{3}$ 0] direction, with a primitive cell of parameters $a = 7.5 \pm 0.8$ Å, $b = 9.5 \pm 1$ Å, and $\gamma = 128° \pm 2°$. Due to the threefold symmetry of the 6*H*-SiC(0001) hexagonal structure, the reconstructed areas can be turned by 120° as shown in Fig. 2(b) compared to Fig. 2(a). There are also antiphase boundaries indicated by white arrows that separate two reconstructed domains in antiphase along the $\langle 1\,0\,\bar{1}\,0\rangle$ axis.

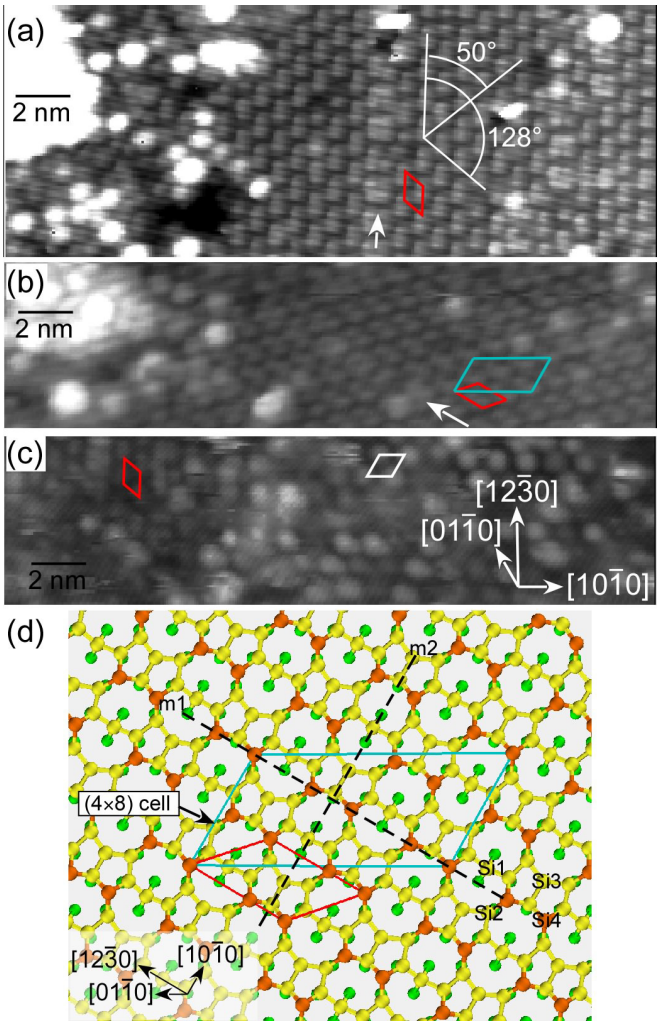

FIG. 2. The (4×8) reconstruction of the Si enriched 6*H*-SiC(0001) surface: (a),(b) Two STM images of 20 nm width of the (4×8) surface and (c) a mixed area with the (3×3) reconstruction (right, white cell) and (4×8) reconstruction (left, red cell). (d) Atomic model of the 6*H*-SiC(0001) (4×8) reconstructed surface relaxed at 300 K. Si4 sp^3 top adatoms are in orange, Si1, Si2, and Si3 adatoms in the first adlayer are in yellow, and the Si surface atoms of the SiC(0001) bulk are in green. The two cells in blue and in red correspond to the ones in (b).

Figure 2(d) presents the atomic model of the reconstruction that remains stable to 1200 K during MD calculations. It involves the same type of Si adatoms that constitute the (12×12) with 7/8 ML of Si1, Si2, and Si3 adatoms and 1/4 ML of Si4 top adatoms. The primitive cell (red) is aligned along the $[1\,\bar{2}\,1\,0]$ and $[2\,4\,\bar{6}\,0]$ vectors, giving the surface cell parameters $a = \sqrt{7}a_{SiC} = 8.19$ Å, $b = 2\sqrt{3}a_{SiC} = 10.72$ Å, and $\gamma = 131°$, in accordance with the experimental values. The blue cell shows the (4×8) cell parallel to the $[1\,0\,\bar{1}\,0]$ and $[0\,1\,\bar{1}\,0]$ directions, chosen to name this reconstruction. The arrangement of the Si4 topmost adatoms presents two orthogonal mirrors [m1 and m2 in Fig. 2(d)] leading to an inversion center, that explains the twofold symmetry of the RHEED pattern. This (4×8) pattern mixed with the (3×3) has been observed by LEED by Xie *et al.* [11], even though these authors have not explicitly reported this [16].

The introduction of the Si1 bridge adatoms is an essential ingredient to build the atomic structure of the two (12×12) and (4×8) reconstructions. We use them to propose improved atomic models for two reconstructions reported in the literature: the $(2\sqrt{3}\times2\sqrt{3})$-$R30°$ [13] and $(2\sqrt{3}\times2\sqrt{13})$ [14,21]. As explained in Ref. [16], the introduction of the Si1 bridge adatoms allows us to propose more stable atomic models of these two reconstructions.

Table I sets out the main information for the six Si-rich surface reconstructions of the 6*H*-SiC(0001) surface: the name found in literature and the associated references, the crystallographic data of the primitive surface cell, the observable RHEED pattern taking into account the symmetry of the surface cell, and the Si adatoms distribution in the different layers.

In the case of a 6*H*-SiC(0001) surface with only one reconstruction, the RHEED patterns obtained in the two $\langle 1\,0\,\bar{1}\,0\rangle$ and $\langle 1\,2\,\bar{3}\,0\rangle$ axis allow us to determine its type without ambiguity. However, it can be difficult for larger cells, such as the (12×12), with numerous fractional streaks of variable intensity. The situation grows complicated in the case of mixed reconstructions. For example a surface with (4×8) mixed with the (3×3) leads to 1/3, 1/2, and 2/3 RHEED streaks in the two $\langle 1\,0\,\bar{1}\,0\rangle$ and $\langle 1\,2\,\bar{3}\,0\rangle$ axis, which can be confused with a (6×6) pattern with weak intensity of the 1/6 and 5/6 streaks. Another situation is the mixed surface $(2\sqrt{3}\times2\sqrt{13})$ and (3×3), which leads to the formation of an improbable RHEED pattern with eight fractional streaks unequally spaced, six from the $(2\sqrt{3}\times2\sqrt{13})$ and two from the (3×3) along the $\langle 1\,0\,\bar{1}\,0\rangle$ axis. These examples demonstrate the difficulty to follow the evolution of the 6*H*-SiC(0001) surface by RHEED or LEED during Si sublimation or enrichment at high temperature.

The Si1 bridge adatoms are present in the four intermediate reconstructions between the Si poor $(\sqrt{3}\times\sqrt{3})$-$R30°$ and the Si rich (3×3) reconstructions. The origin of this bridge configuration can be traced to the mechanism schematized in Fig. 3(a). In the $(\sqrt{3}\times\sqrt{3})$-$R30°$ reconstruction, the Si top atoms are bound to three Si surface atoms of the SiC(0001) surface, reducing the number of dangling bonds by a factor of three. The reaction of an incoming Si atom with an Si top dangling bond will lead to a weakening of one of the back bonds, allowing the insertion of another incoming Si atom. This sequence leads to the situation illustrated on the right of Fig. 3(a) where the Si1 bridge adatom is stabilized by four bounds with neighboring Si atoms. This stable Si1 bridge is surrounded by three Si atoms, engaged in only two bonds, and having two free valence electrons. These three highly reactive Si atoms are then available for the incorporation of incoming Si atoms.

From this mechanism, the obtention of an organized surface depends on the formation of Si-Si bonds with length close to the Si bulk value (2.35 Å). Figure 3(b) shows the Si-Si bond length distribution calculated from the MD models of the (12×12) and the (4×8) reconstructions. The dispersion for the (12×12) is between 2.2 to 2.9 Å with a peak centered at 2.45 Å, while for the (4×8), the range is decreased to 2.2 to 2.6 Å, with a mean value of 2.37 Å close to the Si bulk one. The small increase of 0.125 ML in Si adatoms coverage has an important effect on the bond length distribution. The presence of long Si-Si bonds in the (12×12) can explain its instability at high temperature compared to the (4×8).

TABLE I. Name, crystallographic data, symmetry of RHEED pattern, and details of the Si coverage for the six Si-rich reconstructions of the 6*H*-SiC(0001) surface. In bold font, the coverage of Si atoms in pyramidal top position is indicated for each reconstruction.

Name References	$(\sqrt{3}\times\sqrt{3})$-$R30^\circ$ [1–6]	(12×12)	$(2\sqrt{3}\times2\sqrt{3})$-$R30^\circ$ [13]	(4×8)	$(2\sqrt{3}\times2\sqrt{13})$ [14,21]	(3×3) [4,7–10]
Primitive cell						
$\vec{a}$	[1 2 $\bar{3}$ 0]	[12 0 $\overline{12}$ 0]	[2 4 $\bar{6}$ 0]	[2 4 $\bar{6}$ 0]	[2 4 $\bar{6}$ 0]	[3 0 $\bar{3}$ 0]
$\vec{b}$	[1 $\bar{1}$ 0 0]	[0 12 $\overline{12}$ 0]	[2 $\bar{2}$ 0 0]	[1 $\bar{2}$ 1 0]	[6 $\bar{2}$ $\bar{4}$ 0]	[0 3 $\bar{3}$ 0]
Surface cell parameters						
a (Å)	5.36	37.1	10.72	10.72	10.72	9.28
b (Å)	5.36	37.1	10.72	8.19	22.32	9.28
γ (°)	120	120	120	130.9	103.9	120
Cell along $\langle 1\,0\,\bar{1}\,0\rangle$	(3×3)	(12×12)	(6×6)	(4×8)	(14×14)	(3×3)
RHEED along $\langle 1\,0\,\bar{1}\,0\rangle$	$\times3$	$\times12$	$\times6$	$\times2$	$\times7$	$\times3$
RHEED along $\langle 1\,2\,\bar{3}\,0\rangle$	$\times1$	$\times12$	$\times2$	$\times2$	$\times2$	$\times3$
Si first adlayer (ML)	1/3	7/8	5/6	7/8	25/28	1
Si top atom	**1/3**	0	0	0	0	0
Si1 bridge	0	1/8	1/6	1/8	3/28	0
Si2 + Si3	0	6/8	4/6	6/8	22/28	1
Si second adlayer (ML)						
Si4 top atom		**1/8**	**1/6**	**1/4**	**2/7**	0
Si2 + Si3						1/3
Si 3nd adlayer (ML)						**1/9**
Si total coverage (ML)	1/3	1	1	9/8=1.125	33/28=1.179	13/9=1.444

The fine tuning of the Si coverage is necessary to obtain reproducible 6*H*-SiC(0001) reconstructed surfaces. Except for the transition from the $(\sqrt{3}\times\sqrt{3})$-$R30^\circ$ to the (12×12) reconstruction, the change between neighboring reconstructions requires a rather small change of the total Si coverage. For example only 0.054 ML separates the (4×8) from the $(2\sqrt{3}\times2\sqrt{13})$ reconstruction and 0.265 ML more is necessary to obtain the (3×3). With five reconstructions between 1 and 1.444 ML of Si atoms, it is not surprising to observe mixed reconstructions on the surface.

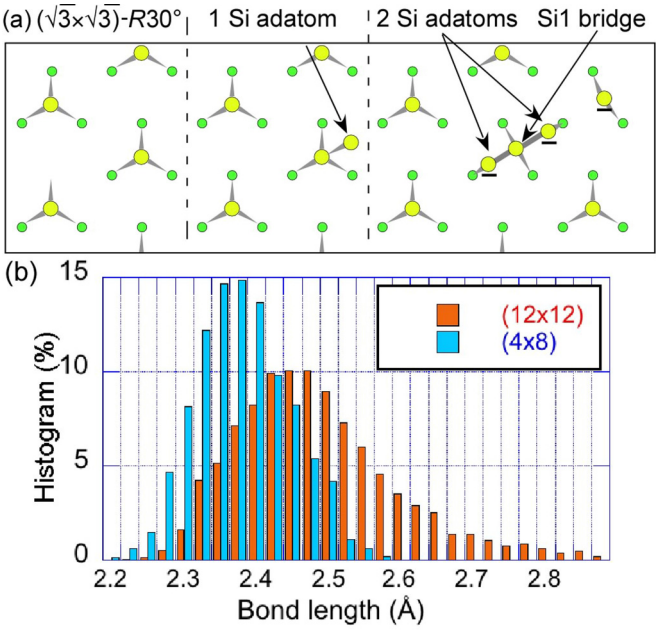

FIG. 3. (a) The addition of two Si adatoms on the $(\sqrt{3}\times\sqrt{3})$-$R30^\circ$ reconstructed surface induces the apparition of a Si1 bridge type adatom. The Si adatoms are in yellow and the Si surface atoms of the SiC(0001) bulk are in green. The black bar below the Si adatoms indicate the presence of two free valence electrons. (b) Distribution of Si-Si bond length calculated from the MD models of the (12×12) (orange bar) and the (4×8) (blue bar) reconstructions.

The reactivity can be evaluated by looking at the coverage of Si top atoms indicated in bold font in Table I. Indeed, these Si top atoms are linked to only three Si atoms and present a dangling bond that is highly reactive with other Si atoms or impurities. With its 1/9 ML Si top atoms, the (3×3) is the less reactive, which can explain its earlier observation. On the contrary, the $(\sqrt{3}\times\sqrt{3})$-$R30^\circ$ with its 1/3 ML of Si top atoms is the most reactive. In between, the four reconstructions show an increasing density of Si4 top adatoms due to the increase of the Si total coverage.

To conclude, we show that the progressive enrichment in Si atoms of the 6*H*-SiC(0001) surface produces two reconstructions: The giant (12×12), stable below $600\pm50\,^\circ$C, and the (4×8), stable at $830\pm50\,^\circ$C. From the atomically resolved STM images, models are built and tested by MD, introducing a type of Si adatom that bridges two Si surface atoms of the 6*H*-SiC(0001) surface. The reconstruction sequence with increasing Si coverage is $(\sqrt{3}\times\sqrt{3})$-$R30^\circ$, (12×12), $(2\sqrt{3}\times2\sqrt{3})$-$R30^\circ$, (4×8), $(2\sqrt{3}\times2\sqrt{13})$, and (3×3). The four middle reconstructions have a Si coverage from 1 to 1.179 ML, which renders them very sensitive to the methods of the SiC surface preparation. This study rationalizes the preparation of 6*H*-SiC(0001) surface, which is of crucial importance to improve its use for elaboration of optoelectronic and high-power electronic devices.

The authors gratefully acknowledge M. Portail for the SiC H_2 gas etching. This work was supported by the Agence Nationale de la Recherche (France) within the project Mol-SiC (Contract No. ANR-08-P058-36 MOLSIC). Part of the calculation was performed using High Performance Computing resources from the Calcul in Midi-Pyrénées (CALMIP) facilities (Grant No. 2011-[P0832]).

[1] R. Kaplan, Surf. Sci. **215**, 111 (1989).
[2] F. Owman and P. Mårtensson, Surf. Sci. **330**, L639 (1995).
[3] L. I. Johansson, F. Owman, and P. Mårtensson, Phys. Rev. B **53**, 13793 (1996).
[4] L. Li and I. S. T. Tsong, Surf. Sci. **351**, 141 (1996).
[5] J.-M. Themlin, I. Forbeaux, V. Langlais, H. Belkhir, and J.-M. Debever, Europhys. Lett. **39**, 61 (1997).
[6] A. Coati, M. Sauvage-Simkin, Y. Garreau, R. Pinchaux, T. Argunova, and K. Aïd, Phys. Rev. B **59**, 12224 (1999).
[7] S. Tanaka, R. S. Kern, and R. F. Davis, Appl. Phys. Lett. **65**, 2851 (1994).
[8] M. A. Kulakov, G. Henn, and B. Bullemer, Surf. Sci. **346**, 49 (1996).
[9] U. Starke, J. Schardt, J. Bernhardt, M. Franke, K. Reuter, H. Wedler, K. Heinz, J. Furthmüller, P. Käckell, and F. Bechstedt, Phys. Rev. Lett. **80**, 758 (1998).
[10] J. Schardt, J. Bernhardt, U. Starke, and K. Heinz, Phys. Rev. B **62**, 10335 (2000).
[11] X. N. Xie, H. Q. Wang, A. T. S. Wee, and K. P. Loh, Surf. Sci. **478**, 57 (2001).
[12] E. Tok, W. Ong, and A. Wee, Surf. Sci. **558**, 145 (2004).
[13] F. Amy, P. Soukiassian, and C. Brylinski, Appl. Phys. Lett. **85**, 926 (2004).
[14] M. Naitoh, J. Takami, S. Nishigaki, and N. Toyama, Appl. Phys. Lett. **75**, 650 (1999).
[15] I. T. Todorov, W. Smith, K. Trachenko, and M. T. Dove, J. Mater. Chem. **16**, 1911 (2006).
[16] See Supplemental Material at http://link.aps.org/supplemental/10.1103/PhysRevB.97.081302 for details on molecular dynamic calculations, SiC substrate preparation, atomic structures of the $(2\sqrt{3}\times2\sqrt{3})$-$R30^\circ$ and $(2\sqrt{3}\times2\sqrt{13})$ reconstructions and LEED observations.
[17] J. Tersoff, Phys. Rev. B **39**, 5566 (1989).
[18] F. Castanié, L. Nony, S. Gauthier, and X. Bouju, Beilstein J. Nanotechnol. **3**, 301 (2012).
[19] H. Okumura, M. Horita, T. Kimoto, and J. Suda, Appl. Surf. Sci. **254**, 7858 (2008).
[20] D. Martrou, L. Guiraud, R. Laloo, B. Pecassou, P. Abeilhou, O. Guillermet, E. Dujardin, S. Gauthier, J. Polesel-Maris, M. Venegas de la Cerda, A. Hinaut, A. Bodin, F. Chaumeton, A. Piednoir, H. Guo, and T. Leoni, in *Atomic Scale Interconnection Machines* (Christian Joachim, Berlin, Heidelberg, 2012), Springer ed., pp. 35–52.
[21] L. Li, Y. Hasegawa, T. Sakurai, and I. S. T. Tsong, J. Appl. Phys. **80**, 2524 (1996).